*JAKU: Earth Sci.,* **Vol. 23,** No. 1, pp: 1-21 (2012 A.D. / 1433 A.H.)

DOI: 10.4197 / Ear. 23-1.1

# Delineation of Saltwater Intrusion in Al Makha Area, Red Sea Coast, Yemen, Using Electrical Resistivity Measurements

**Ahmed A. Abdulqader** and **Mahmoud M. Senosy**[1]

*Geology Department, Taiz University, P.O.Box 6803 Taiz, Yemen*
*[1]Geology Department, Assuit University, Egypt*

*Email: drahaziz@yahoo.com* *Email: mmsenosy@yahoo.com*

Received: 10/03/2010 Accepted: 16/02/2011

*Abstract*. Al Makha is an ancient and important port in Yemen. It is confronted with a dramatic shortage of fresh water supply because of groundwater contamination by sea water intrusion. To study this problem, two dc-resistivity methods, vertical electrical sounding (VES) and two dimensional 2D resistivity imaging surveys, have been conducted. Ten VES-es were preformed in the alluvial plain area and four 2D-resistivity profiles were conducted in the coastal strip near the shore line.

Interpretation of the collected resistivity data, correlating with water depth and electrical conductivity measurements revealed the presence of two water bearing horizons, the upper is correlated to medium to coarse-grained sands intercalated with clay, extends from the surface to 30 and 85 m depth with average thickness of 50 m. The lower is correlated to medium to fine-grained deposits extends to about 250 m below the mean sea level. A combined surface resistivity and hydrochemical data indicate invasion of the Red Sea water into the lower alluvial aquifer. The saline water saturated zone is shallow near the shore line and goes deeper inland. The depth to the top of saline water intrusion is about 10-m at 2-km distance from the shore and increased to 150 m at 10 km. Also, it extends in a zigzag line parallel to the shore line depending on the morphology of the seawater, subsurface geology, and rate of pumping. Water table contours of the aquifer showed that the groundwater flow does not have a definite direction but it depends on the abstraction rate over the area.

## Introduction

Investment of the Tihama coastal plain is the most important strategic objective of the Yemeni government. However, saline water intrusion and fresh water shortage become the major environmental problems that threaten groundwater resources and future development in the coastal area. Due to its important and strategic position, the present study is focused on the Al Makha area, a large number of wells have been abandoned or became saline. Moreover, many farmers left their coastal lands and drilled new wells inland.

Since the early 1970s, many government agencies have been created to investigate groundwater resources in Tihama plain (such as El-Eryani, 1979, DHV, 1983, Gun and Ahmed, 1985, DHV, 1986 and 1988, TS-HWC, 1992 and Rybakov and Tkachenko, 1995). Most of these studies were focused on the groundwater resources in the central and northern areas. However, the hydrogeology and contamination by saline water intrusion in southern areas are still unknown.

Resistivity varies according to small changes in water salinity, this property together with the low cost make the direct current resistivity methods very suitable for groundwater investigation. Among these methods, the vertical electrical sounding VES and two dimensional 2D resistivity imaging techniques are preferentially used to study the groundwater conditions of the coastal aquifers (*e.g.* De Breuk and De Moor, 1969, Ebrahem *et al.,* 1977, Van Overmeeren, 1989, Zohdy *et al.,* 1993, Griffiths and Barker, 1993, Urish and Frohlich, 1990, Frohlich *et al.,* 1994, Dahlin, 1996 and Nowrooz *et al.,* 1999).

In the present study, the two mentioned techniques were applied to supplement the lack of geological and hydrological information. The 2D-resistivity imaging was performed in the coastal area, where the saline water saturated zone is expected to be at shallow depth while the VES was used for deeper exploration in the alluvial plain area. A combined geoelectrical, hydrochmical, and well observations data were integrated to delineate the saline water intrusion and the geometries of the aquifers.

## 2. The Study Area

### *2.1. Area Description*

The study area lies in the southwestern Tihama plain on the Red Sea at about 80 km SW of Taiz city (13° 25`–13° 30`N and longitudes

43° 25`– 43° 40` E, Fig. 1), covering an area of approximately 70 km$^2$, with a total population of about 20,000 inhabitants (Yemen National Census, 2004). The study area is nearly flat but gently sloping towards the sea, with elevation ranges from 0 and 60 m above mean sea level.

Geomorphologically, the area can be divided into two units; 1) coastal strip, and 2) alluvial plain. The first is developed along the shore line of 3-km width. It includes elongated barrier island, salt marshes, coastal sands and sand dunes. The alluvial plain extends eastward. It is composed of alluvial deposits dissected by older flood channels and covered with some halophyte vegetation.

The climate in the area under investigation can be described as being hot, windy and arid. The monthly temperature ranges between 25°C (as minimum in January) and 37°C (as maximum in July), with average monthly humidity of 60-75%. The annual rainfall is generally very low (<50 mm/year). As there is no desalinization plants, groundwater is the main source for drinking domestic use and irrigation. Groundwater abstraction was estimated to be 2.5 Mm$^3$/year, through about 40 shallow wells of 10 to 100 m deep. Most of abstracted water is used for irrigation, and only about 0.3 Mm$^3$/year is used as drinking water supply for Al Makha city.

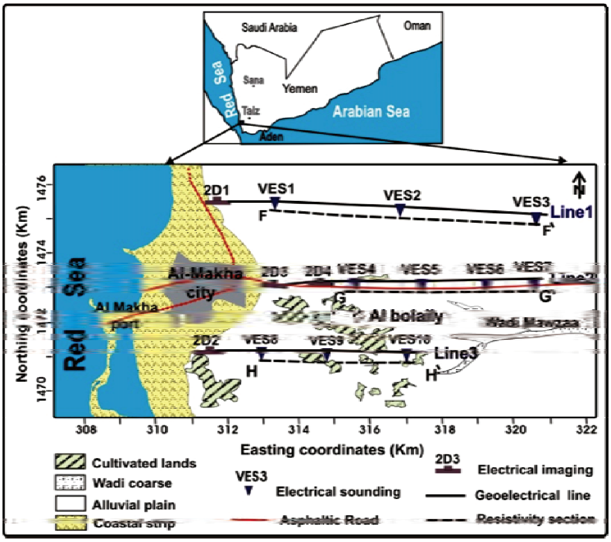


**Fig. 1.** **Map showing the study area including surface features, locations of resistivity measurements (2D-profiles and VES sites).**

## *2.2. Geological and Hydrogeological Background*

The regional geology of the area is adopted from the previous studies undertaken in Tihama coastal plain (*e.g*. Geukens, 1966, Van Overmeeren, 1985, DHV, 1983 and 1986 and TS-HWC, 1992). The area is covered by Recent aeolian/alluvial deposits and sedimentary debris. The subsurface geology is built up of a thick sequence of clastic sediments, overlying a down faulted surface of consolidated bed rock. The clastic sediments comprise two units, the upper Quaternary unit rests unconformably on the lower Tertiary unit (DHV, 1986). A schematic geological cross-section is presented in Fig. (2). The upper Quaternary unit consists of three layers; from top to bottom, Recent aeolian/alluvial deposits, range from 3 m thickness near the shore to 30 m in the east, Recent to Quaternary alluvial/aeolian sediments, with maximum thickness of about 100 m and Quaternary alluvial/aeolian sediments, with maximum thickness of about 350 m. The lower Tertiary sediments are formed of fine deposits of the Baid Formation, a succession of alternating clays, silts, fine sand, evaporites, and partly cemented weathered volcanics (DHV, 1986). The thickness of this layer ranges from several hundred meters to three kilometers (TS-HWC, 1992).

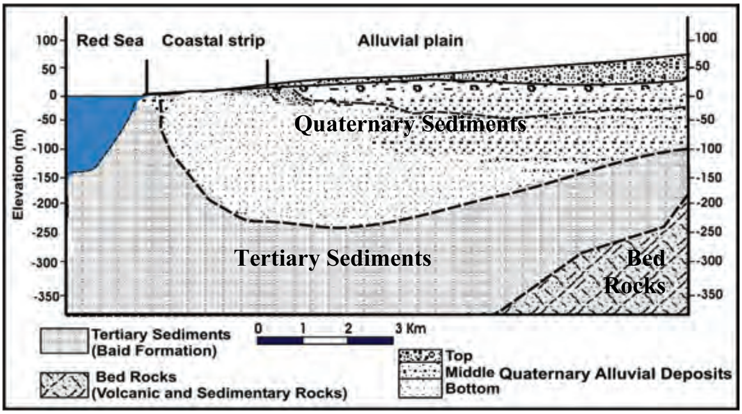


**Fig. 2. Schematic lithostratigraphic cross section of Al Makha area, Tihama, Yemen**.

Hydrogeologically, the most important aquifer in Tihama is the Quaternary alluvial deposits that was classified into two aquifers - an upper, which is more permeable sequence up to 70 m thick, and a lower, which is more consolidated or finer grained sequence of lower permeability to depths of 250 m or more (TS-HWC, 1992). The hydraulic conductivity (K) of 30-40 m/d were common up to 100 m depth, and the transmissivity (T) values in the aquifer increase westward from 1000 $m^2$/d in the central part of the plain to 3000 $m^2$/d near the coast. The specific capacity values range between 3 and 8 l/s/m with specific yield of about 7 to 23% (DHV, 1988). The water table occurs under unconfined condition; the aquifer is mainly recharged by subsurface inflow from the surrounding areas, and discharged naturally by evaporation and evapotranspiration, and artificially by abstraction through the shallow wells.

## 3. Methodology

### *3.1. Field Measurements*

This study is based on the previous regional geological and hydrogeological information; the electrical resistivity surveys and well inventory acquired by the authors between July/2006 and June/2007. The VES and 2D-resistivity imaging were applied for this investigation. Three parallel investigated lines (Line1, Line2, and Line3, Fig. 1), oriented W-E, with 6 - 9 km length and 2 km apart, and are distributed along the survey area. The VES are used to define the geometries of the different aquifers, and to map the fresh water lenses. The 2D resistivity profiles were arranged close the shore line. The data were collected by using the ABEM, SAS 1000 instrument.

Vertical electric sounding (VES) survey was performed at ten points distributed along three profiles crossing the alluvial plain area. The VES stations were distributed, at 2-4 km intervals, along the profiles FF`, GG`, and HH`. Schlumberger electrode configuration was used for data acquisition with maximum current electrode separation (AB/2) 500 m, and potential electrodes (MN/2) varied from 0.5 m to 30 m. It was not possible to conduct soundings in some areas covered with high resistive piedmonts, or dense trees. The VES field measurements, including electrode separation, and apparent resistivities $\rho_a$ for each sounding are listed in Table (1).

Four 2D profiles (2D1, 2D2, 2D3, and 2D4) were conducted close to the sea, where saline water is considered to be at shallow depth, with the purpose of mapping saline water intrusion near the shore line. The Wenner–Schlumberger on linear electrode arrays was used for data acquisition. The lengths of profiles range between 180 and 240 m and a number of 37 to 48 electrodes with smallest electrode spacing 5 m.

**Table 1. Field measurements for 10 VESs in Al Makha area, Red Sea coast, Yemen.**

| AB/2 (m) | MN/2 (m) | VES no. | | | | | | | | | |
|---|---|---|---|---|---|---|---|---|---|---|---|
| | | 1 | 2 | 3 | 4 | 5 | 6 | 7 | 8 | 9 | 10 |
| 1.5 | 0.5 | 7 | 47.6 | 139 | 54.6 | 50 | 311 | 278 | 6.9 | 217 | 129 |
| 2 | | 7.5 | 36.2 | 121 | 45.8 | 37.6 | 328 | 254 | 6 | 189 | 113 |
| 3 | | 7.8 | 31.7 | 115 | 37.5 | 27.5 | 253 | 196 | 4 | 76.3 | 80.6 |
| 5 | | 8.6 | 24.5 | 89 | 29.4 | 30.3 | 140 | 110 | 5 | 37.7 | 49 |
| 7 | | 6.5 | 16.7 | 56 | 21.7 | 30 | 102 | 51 | 5.7 | 26 | 32 |
| 10 | | 5.5 | 14.5 | 34 | 15 | 42 | 110 | 25.5 | 7 | 23 | 25.4 |
| 10 | 1 | 5.5 | 14.5 | 35 | 14.5 | 43 | 110 | 29.2 | 7 | 23 | 26.8 |
| 15 | | 7.8 | 14.9 | 29 | 12.2 | 54 | 133 | 19 | 7.2 | 25 | 25.3 |
| 20 | | 9.9 | 18.5 | 30 | 16.5 | 59 | 145 | 19.4 | 8.2 | 25 | 32.5 |
| 25 | | 10.8 | 20.8 | 25 | 21 | 57.8 | 126 | 21.6 | 8.5 | 24 | 38 |
| 30 | | 11 | 23.3 | 22 | 21 | 56.6 | 107 | 23 | 9 | 23 | 45 |
| 30 | 3 | 11 | 23 | 22 | 21.4 | 56 | 107 | 23 | 9 | 23 | 45 |
| 40 | | 9 | 23.3 | 26 | 25.3 | 47.8 | 79 | 22 | 10 | 17 | 43.6 |
| 50 | | 8 | 21.3 | 30 | 30 | 51 | 64 | 24 | 12 | 12 | 39 |
| 70 | | 10 | 20.7 | 36 | 35 | 41 | 36 | 24 | 14 | 11 | 32 |
| 70 | 10 | 10 | 20.6 | 36 | 34.6 | 41 | 36 | 21 | 14 | 11 | 32 |
| 100 | | 11 | 18.6 | 26 | 27 | 35 | 26 | 22 | 17 | 13 | 25 |
| 125 | | 10 | 18.4 | 23 | 26 | 25 | 18 | 19 | 18 | 18 | 20 |
| 150 | | 8.3 | 16 | 22 | 25 | 23 | 16 | 15 | 17 | 18 | 15 |
| 175 | | 7.5 | 15 | 21 | 23 | 20 | 17 | 13 | 16 | 18 | 15 |
| 175 | | 7.2 | 15.5 | 20 | 21.5 | 19 | 17 | 12 | 16 | 18 | 15 |
| 200 | | 7 | 13.8 | 19.5 | 17.6 | 18.5 | 17 | 12 | 13 | 16 | 12 |
| 250 | | 7 | 13.9 | 19.5 | 13 | 19 | 19 | 10 | 9 | 13 | 12.5 |
| 250 | 40 | 7.5 | 13.7 | 17.6 | 13.5 | 19 | 18 | 7 | 8 | 11 | 11 |
| 300 | | 6 | 13 | 16 | 12.8 | 16 | 16 | 7 | 8 | 11 | 11 |
| 400 | | - | - | 15 | 7.1 | 12.4 | 16 | - | - | - | - |
| 500 | | - | - | - | - | 11.2 | 9.7 | - | - | - | - |

To complement the results of resistivity survey, total dissolved solids TDS of groundwater samples and water level measurements were used to differentiate between fresh, brackish, and saline water. Depths to water table were measured for 34 wells distributed over the area, groundwater table with respect to mean sea level was contoured to construct water table map. The Electrical Conductivity (EC) for the collected water samples was measured. Of these, ten water samples were analyzed for pH, chlorides, sulfate, magnesium, calcium and alkalinity.

### *3.2. Data Processing and Interpretation*

The field geoelectric data were processed and interpreted automatically by using the IPI2-win computer program (Geoscan-M, 2001). Results of these interpretations classified the investigated subsurface sequence into three to six successive geoelectric zones of different resistivity ranges, thicknesses and depths. The results (true resistivities ρ and thicknesses T) for each VES station, including the depths to the top of saltwater intrusion are given in Table (2). A representative example of the automatic interpretation of VESs using IPI2win is shown in Fig. (3).

The vertical electrical sounding data were also evaluated using an automatic technique (Zohdy, 1989) to invert the observed data in terms of vertically layered earth model. The layer parameters of one-dimensional model (resistivity and thickness of each layer) and field data for the soundings along each line are entered to the SURFER program (Golden Software, 1994) and contoured in the form of a true resistivity section.

**Table 2. Interpretation results using IPI2win (Geoscan-M, 2001); ρ1, ρ2, ρ3 are resistivities of top, middle and bottom zones; T1, and T2, thicknesses of top and middle zone.**

| VES no. | Profile | True resistivity Ωm | | | Thickness (m) | | Depth to saltwater (m) |
|---|---|---|---|---|---|---|---|
| | | ρ1 | ρ2 | ρ3 | T1 | T2 | |
| 1 | FF` | 7 | 11 | 5 | 10 | 69 | 75 |
| 2 | | 5-500 | 17 | 10 | 10 | 75 | 140 |
| 3 | | 24-139 | 20 | 13 | 37 | 45 | ? |
| 4 | GG` | 5-394 | 15 | 6 | 15 | 57 | 100 |
| 5 | | 20-138 | 20 | 7-15 | 29 | 29 | 190 |
| 6 | | 24-533 | 13 | 7-20 | 32 | 26 | 200 |
| 7 | | 16-45 | 18 | 11-3 | 34 | 31 | 150 |
| 8 | HH` | 2-11 | 51 | 3 | 21.6 | 39 | 130 |
| 9 | | 4-360 | 68 | 6 | 30 | 31.4 | 140 |
| 10 | | 6-125 | 175 | 11 | 4.5 | 7.5 | 100 |

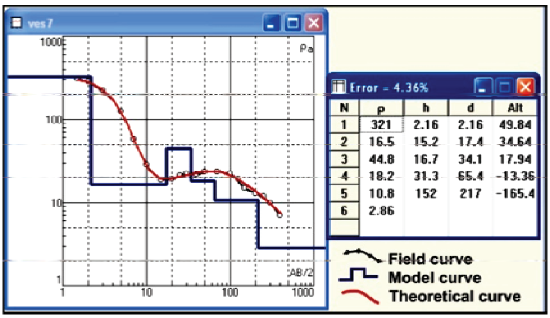


**Fig. 3. An example of inversion results of IPI-2win for sounding VES7; showing digitized field curves, subsurface model, and theoretical curve based on models.**

The 2D–resistivity data were processed using the Res2dinv resistivity inversion software. The least-squares inversion method was applied to invert apparent resistivity data from the field into two-dimensional resistivity earth models. The inverted data were displayed in the form of 2D-resistivity cross sections.

### *3.3. Geoelectrical Calibration Model*

For layer containing water, resistivity obtained by the inversion process is controlled by the resistivity of the pore water and the resistivity of the host rock. The specific resistivity of the layer $R_b$ is expressed as: $R_b = F.\ R_w$; where $F$ is the formation factor, $R_w$ is the resistivity of groundwater. The formation factor F depends on the porosity, sorting, clay content, and the degree of consolidation or cementation of the sediments. The resistivity of water $R_w$ may vary from 0.2 (seawater) to over 1000 Ωm depending on its ionic concentration and the amount of dissolved solids (Nowroozi *et al*., 1999). Resistivity of groundwater and sediments without clay may vary from 1 to 100 Ωm, while resistivity of wet clays alone may vary from 1 to 120 Ωm (Parasnis, 1986). The resistivity of a layer saturated by saline water and some dissolved solids is in the range of 8 to 50 Ωm (De Breuk and De Moor, 1969, Goodell, 1986, Flanzenbaum, 1986, and Zohdy *et al.,* 1993).

Based on previously published geoelectric studies, conducted in similar subsurface conditions (*e.g.* Nowroozi *et al.,* 1999); and the regional geoelectrical model of Tihama (DHV, 1986). A modified geoelectrical model is developed (Table 3), and used as a guide for the interpretation of resistivity data in the present study. Accordingly, subsurface of the study area were subdivided into the following zones: (a) the top geoelectrical zone of high resistivities (>70 Ωm) is correlated with the surfacial dry coastal sands and plain deposits, (b) the geoelectrical zone of 30 - 70 Ωm is correlated to unsaturated upper Quaternary deposits, (c) the geoelectrical zone of 15 - 30Ωm is correlated to upper Quaternary deposits saturated with brackish water, (d) the geoelectrical zone of 10 - 20 Ωm is correlated to the lower Quaternary alluvial deposits saturated with brackish water, and (e) saline water saturated zone is interpreted as the zone having low resistivity (5 - 12 Ωm) at shallow depths and with very low resistivity (< 5 Ωm) at deeper zones. The top surface of the saltwater intrusion is considered to be the 10 Ωm over the whole of study area.

**Table 3. Geoelectrical model of Al Makha area (modified after DHV, 1986).**

| Layer | sediments | Average formation factor F | EC range (µS./cm) | Sp.resistivity $R_b$ (Ωm) | Interpretation |
|---|---|---|---|---|---|
| **upper Quaternary alluvial/aeolian sediments** | Sand gravel, with clay intercalations | 2.5 | <1500 | 20- 50 | fresh water aquifer |
| | | | 1500-2500 | 12 - 20. | brackish water |
| | | | >2500 | <12 | salty water |
| **Lower Quaternary** | Sand, silts, minor clay | 2.3 | <2000 | 15- 25 | fresh water aquifer |
| | | | 2000-3000 | 8 - 15. | brackish water |
| | | | >3000 | <8 | salty water |
| **Transition zone near the shore line** | fine sands, some evap-orates grains | 2 | >2500 | 10 - 15. | poor quality fresh water |
| | | | 2500-4500 | 5-10. | brackish water |
| | | | >4500 | <5 | salty water |

## 4. Results and Discussions

### *4.1. Groundwater Level and Flow*

As shown in groundwater level map (Fig. 4), water level ranges between 32 m (above mean sea level) and -10 m (below mean sea level). The highest water level (32 m) is measured in the south eastern part, at the downstream of Wadi Mawzaa, and the lowest value (-10 m) is measured in the central part (Al bolaily), where groundwater is extensively extracted for irrigation. This may initiate off-shore seepage of saline water from the sea, coastal marshes, salt lakes, and continuously eastward within inland aquifer. Water table configuration of the area shows a wide variation in hydraulic conductivity of the aquifer due to varied lithological conditions and pumping rate. Convergence of hydraulic gradients towards the central area is suggestive of extensive pumping and increase of permeability of the shallow aquifer. The general flow was from the downstream of Wadi Mawzaa in the southeastern part and from the Red Sea towards extensive pumping area in the central part.

### *4.2. Hydrochemistry of Groundwater*

The measured Electric Conductivities (EC) were converted into Total Dissolved Solid (TDS), using the relation, TDS = 0.65 EC (Hem, 1989), and represented as salinity distribution map. The field measurements for the ten water samples collected from the study area (Table 4) show a wide variation of salinity. The water samples in the study area were classified into; 1) slightly fresh water (TDS < 1500 (mg/l), 2) brackish water (TDS 2000-3000 mg/l), and 3) saline water (TDS > 3000 mg/l). As shown in water salinity map (Fig. 5), saline water zone occurs in the coastal strip and extends as a zigzag line parallel to the shoreline. The brackish water zone (TDS 3000-2000 mg/l) cover the middle part of the area, and extends to about 8-km in the northern and southern part. Fresh water of TDS < 1500 mg/l was found in the highly discharging area, as in Al Bolaily (TDS = 957 mg/l, sample W7), while saline water were found near the shore (TDS = 4640 mg/l, sample W2). Varied extension of saline water zone may due to the pumping rate variation, which increased or decreased the groundwater movement and/or perhaps related to the morphology of the sea. Generally, the groundwater of Al Makha area is slightly brackish, with TDS > 1500 mg/l, pH from 7.3 to 9. The remarkable increase in TDS as water runs off towards the shore line is ascribed to evaporation, long flow path, dissolution of evaporate grains in lower alluvial aquifer, and to saline water intrusion from the sea.

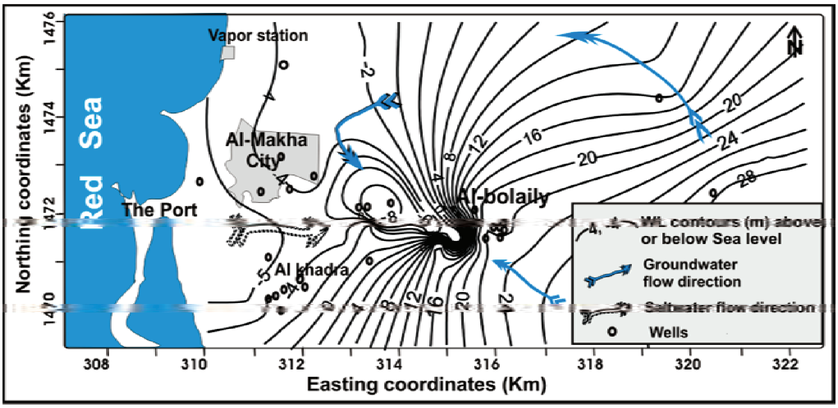


**Fig. 4. Groundwater level map showing pattern and direction of groundwater flow.**

**Table 4. Field measurements data for groundwater samples collected from study area.**

| Monitoring wells | W1 | W2 | W3 | W4 | W5 | W6 | W7 | W8 | W9 | W10 |
|---|---|---|---|---|---|---|---|---|---|---|
| Altitude (m)a.m.s.l. | 3 | 2 | 3 | 12 | 14 | 21 | 23 | 23 | 25 | 45 |
| Depth to water (m) | 5 | 6.5 | 6.5 | 18 | 26 | 27 | 33 | 32 | 40 | 32 |
| EC µS/cm | 6012 | 7140 | 3000 | 3060 | 3560 | 2420 | 1473 | 1980 | 1700 | 1760 |
| TDS (mg/l) | 3907 | 4640 | 1950 | 1990 | 2314 | 1586 | 957 | 1289 | 1100 | 1144 |
| pH | 7.7 | 7.3 | 9 | 7.9 | 7.7 | 7.5 | 7.6 | 7.6 | 7.4 | 7.9 |

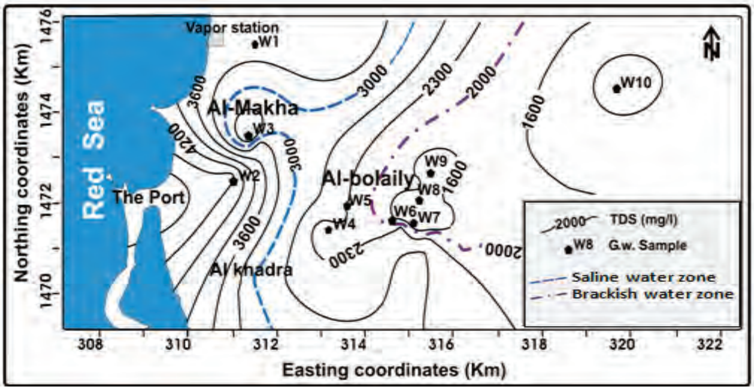


**Fig. 5. Distribution of total dissolved solids in the study area.**

## *4.3. Geoelectrical Results*

### *4.3.1. The Vertical Electrical Sounding Data*

There is a general decrease in the apparent resistivities with increases AB/2, as shown in Table (1). The apparent resistivity values range between 5 and 328 Ωm at 1 - 50 m current electrode spacing, then resistivity decrease to range between 10 and 64 Ωm at 50 - 200 m current electrode spacing, and then decrease to 7 - 12 Ωm at maximum spacing of 500 m. Soundings located in the coastal zone (VES1, and VES8) reveal apparent resistivities of 6 - 15 Ωm for all electrode sapcings. Most of the field curves are of *Q, or HK*-types, they depicted a three or four subsurface layers having resistivities ($\rho_a$) decrease with depth.

### *4.3.2. 2D-Resistivity Profiles*

The inversion results of 2D-resistivity survey are shown in Fig. (6a, 7a, and 8a). Overall pattern of the resisivity images showed three major resistivity zones; from top to bottom, high resistivity zone (> 30 Ωm), intermediate resistivity zone (10 – 30 Ωm), and low resistivity zone (< 10 Ωm). In these sections, the very low resistivity zones (<5 Ωm) is considered as a saline water saturated zone, intermediate resistivity zones is interpreted as fine coastal sands or top soils. High resistivity zones were considered as unsaturated alluvial deposits. The upper parts of the images 2D1 and 2D2 (Figs. 6a and 8a) are dominated by intermediate to high resistivity (10 - >77 Ωm), with thickness range from 11 m in the west to 22 m in the eastern ends of the profiles. This zone is underlined by very low resistivity zone (< 5 Ωm) down to the bottom of the image.

On the contrary, profiles 2D3 and 2D4, which are located at greater distance from the shore, show that the upper part of the images are dominated by intermediate resistivity zones (10 - 30 Ωm), with thickness range between 20 m (in profile 2D3) and 10 m (in profile 2D4), underlined by high resistivity zones of (25 - 70 Ωm) down to the bottom (in the image 2D3). Low resistive zone is observed at depth of about 35 in the image 2D4 (Fig. 7a), this is interpreted as the alluvial deposits saturated with brackish water.

### *4.3.3. Resistivity Cross Sections*

Three resistivity cross sections (Fig. 6b, 7b, and 8b) were obtained by contouring the n-layer models for the soundings located along each resistivity profile. The sections, FF\`, GG\`, and HH\`, are used to differentiate between fresh, brackish, and saline water zones. In all cross-sections, high resistivity value contours (> 70 Ωm, hachured zones) represent the upper unsaturated alluvial deposits while the 60-value contours represent the freshwater table, the 40-value contours represent the fresh/brackish water interface, and the top of saltwater interface is represented by 10-value contour lines.

The section FF\` starts at VES1 and ends at VES3, with a total length of about 8 km and crosses the northern area (Fig. 6b). It shows that the top of saltwater intrusion extends from a shallow depth (70 m below VES1) to a depth of about 150 m (at VES2), it may extend eastward more than 150 m. Section GG\` starts at VES4 and ends at VES7, it has a total length of about 6 km crossing the middle area (Fig. 7b). This section shows that the top of the saltwater intrusion is deeper than that in FF\` section, the 10 Ωm contour starts from a depth of 130 m (below VES4) to 200 m depth in central part at 4-km mark, then tends to become at shallower depth of 150 m at the end of the section (below VES7). Section HH\` starts at VES8 near the coast and ends at VES10, it has a length of about 6 km (Fig. 8b). This section shows the same feature as that in section GG\` but the 10-value contour is slightly shallower.

From the three sections, it can be concluded that the saltwater interface is located at shallower depths near the shore and deepens toward the east. The depth to the top of saltwater zone ranges from 75 to 130 m at 3-km distance from the shore line, and extends to about 200 m depth at the end of the sections. Also the saline water intrusion is deep in the southern part of the area, and tends to be shallower northward.

### *4.3.4. Geoelectrical Cross Sections*

Correlating the 2D-resistivity sections and 1D inversion models with geological data and field observations, three geoelectrical cross-sections have been constructed (Fig. 6c, 7c, and 8c), and used to delineate subsurface lithology, aquifer geometries, and lateral and vertical extent of saline water intrusion.

By inspection of the geoelectrical cross-sections, three main resistivity zones have been identified. The first extends from the ground surface to depth that ranges from 4 m near the shore to 34 m in the eastern margin of the area (below VES7, Line2; Fig. 7c). It has resistivity varies from 7 to 500 Ωm, depending on the moisture content and grain size of the deposits. The lowest resistivity values were found in the coastal strip, considered as salty fine-sediments, the highest values were observed in the eastern part of the plain, where sediment debris prevail. This zone represents top unsaturated or weathered zone, which is composed of dry fine coastal-sand in the coastal part, dry (occasionally wet) soils, sand and gravels of different grain sizes intercalated with clay lenses and rock debris in the eastern part.

The second geoelectric zone extends from the base of the first geoelectric zone, with a thickness ranges from 30 m in the coastal part (below 2D2, VES8, Line1; Fig. 8c) to 69 m (below VES1, Line1; Fig. 6c), it increase in thickness northward and eastward. Its resistivity values range between 5 and 175 Ωm above the water table, and between 11 and 68 Ωm below the water table. The low resistivity value is attributed to the fine-grained sediments of the coastal sands, and/or due to brackish water saturation. The zone is correlated with the upper alluvial deposits, which is represented as the main groundwater aquifer. Free groundwater levels decreased from 22 m in the southeastern part of the area (near VES7 and VES10; Fig. 7c, and 8c) to -4 m in the western-central area (between VES5 and 2D3, line 2; Fig. 7c). The resistivity values of this zone indicate that the brackish water is found in the northern and southern parts of the area, slightly fresh water in the central highly exploited area.

The third geoelectric zone underlies the second one and extends to a depth of greater than 250 m from the surface. This zone is interpreted as fine-grained alluvial sediments. It has low resistivity all over the area, the resistivity values range from less than 2 Ωm (below 2D1, Fig. 6a) to maximum 20 Ωm in the eastern part. The low resistivity values of this zone suggests different groundwater salinities, ranging from saline water of <5 Ωm in the west to brackish (5- 10 Ωm) in the middle, and (10- 20) in the eastern part. The depth to the saltwater surface ranges from 10 m at 2 km distance from the sea (below 2D1 and 2D2; Fig. 6c and 8c) to 40 m at 4 km distance. In the alluvial plain area, the depth to saline water range from 70 m at 3 km mark distance from the shore to 150 m at 11-km . Along line2 (the central part, Al bolaily area) depth to saltwater is found at relatively greater depth (about 200 m).

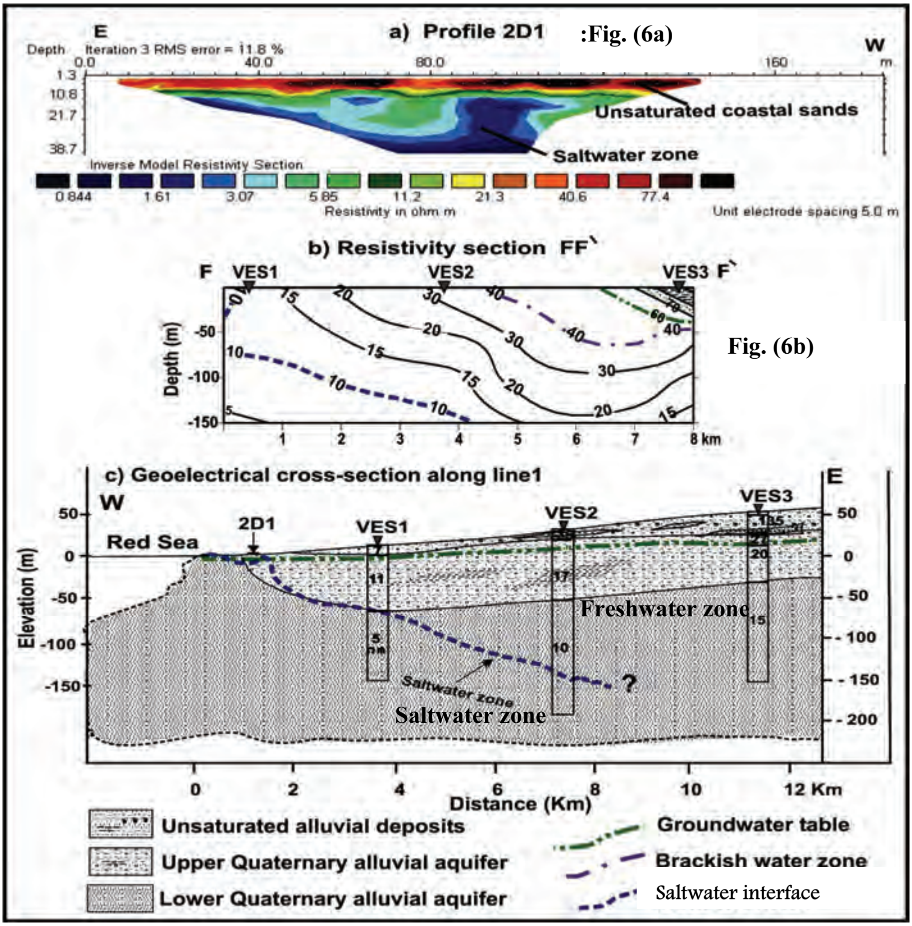


**Fig. 6 (a, b, and c): a) 2D-resistivity section of profile 2D1, b) resistivity cross-section FF`, and c) geoelectrical cross-section along the resistivity survey line1, based on 2D and VES inversion results, showing the depth of water table and depth and extent of saline water interface along the northern part of study area.**

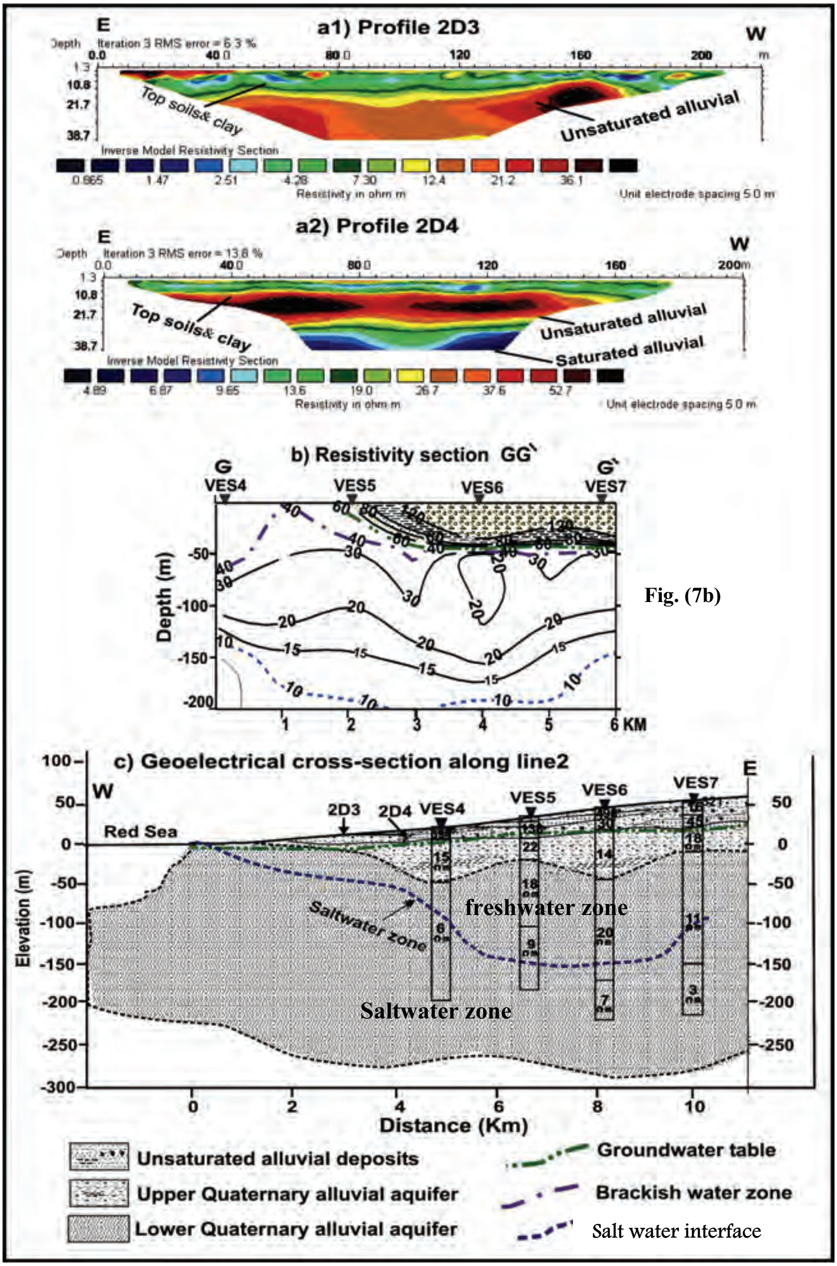


**Fig. 7 (a, b, and c): a) 2D-resistivity section of profile 2D3 and 4, b) resistivity cross-section along GG`, and c) geoelectrical cross-section along the resistivity survey line2, along the central part of the study area.**

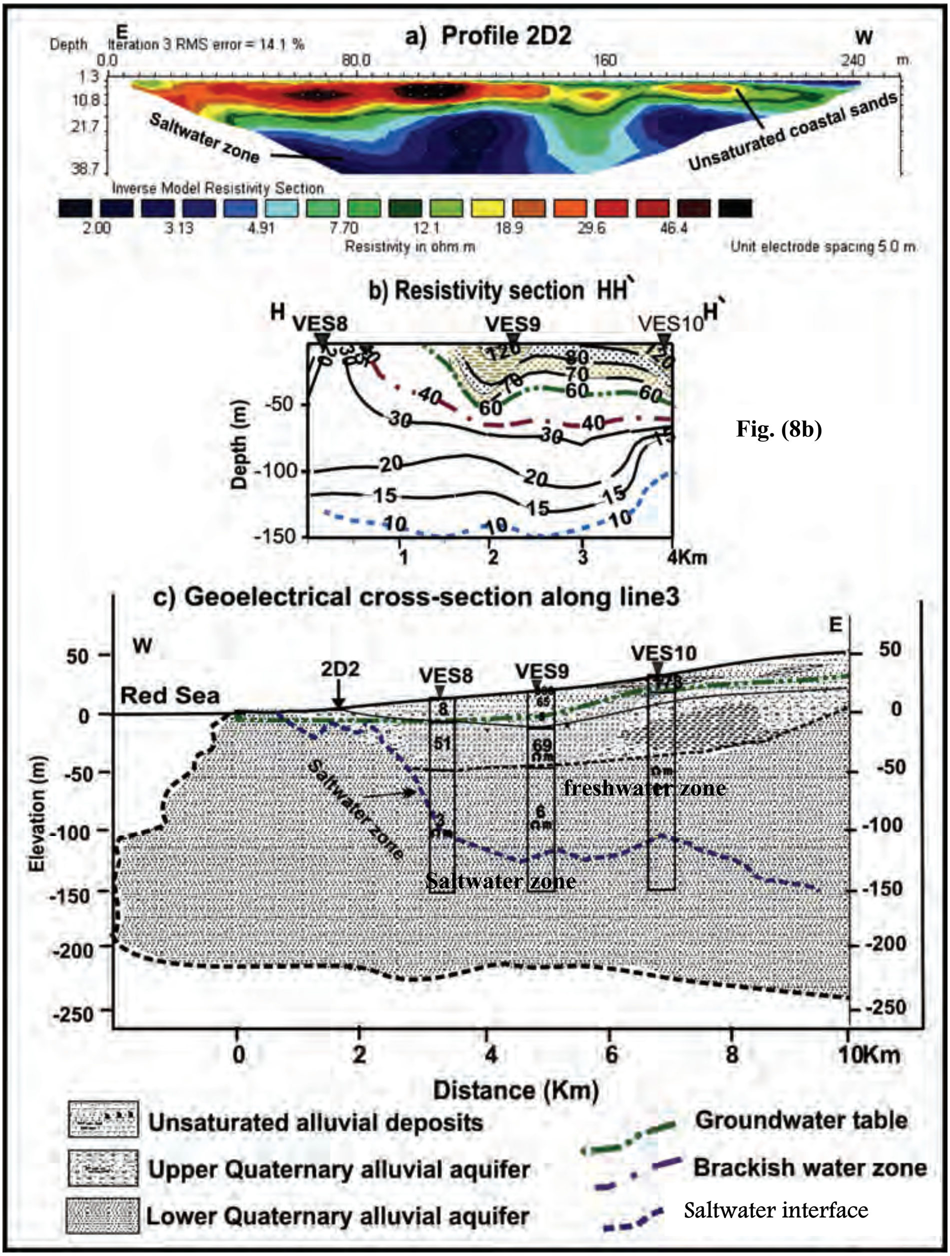


**Fig. 8 (a, b, and c): a) 2D-resistivity section of profile 2D2, b) resistivity cross-section along HH`, and c) geoelectrical cross-section along the resistivity survey line3, along the southern part of the study area.**

### *4.4. Delineation of Saline Water Intrusion*

The extent of seawater intrusion within the aquifer system of the study area was investigated by correlating the 2D-resistivity sections and VES models. Inversion results indicate that the saline water invades the lower aquifer, which has direct contact with it. The depth to the top surface of seawater intrusion ranges from 10 m near the shore line to more than 150 m in the eastern end. The saline/brackish water interface, however, is located within the lower Quaternary aquifer, it is found at shallower depth near the shore, and deepens towards the east and south. This may be due to either increasing of fresh water accumulation in this direction or decreasing the permeability of aquifers in these parts.

## 5. Conclusion

In the present study, vertical electrical sounding (VES) and two dimension (2D) resistivity imaging have been used to investigate the hydrogeology of Al Makha area, Tihama coastal plain, Yemen. The resulting geoelectric information, coupled with hydrological and hydrochemical data, have successfully delineated the saltwater intrusion within the coastal aquifer system, and identified the aquifers conditions of the area from the surface to about 250 m depth.

Two alluvial aquifers have been identified; an upper aquifer of coarser grain size sediments intercalated with fine sands and clays, its surface and subsurface develop slightly in the alluvial fan of main wadi channels, with thickness ranges between 30 and 80 m. The aquifer is recharged from the floods, and extensively discharged through pumping; it contains relatively good water quality. Below, a lower aquifer is formed by medium-to-fine alluvial sediments, with thickness more than 250 m. this aquifer is well developed throughout the Tihama plain until it exceeds the boundary with the Red Sea.

The surface resistivity and hydrochemical data indicate invasion of the Red Sea water into the lower alluvial aquifer while the upper is not affected by seawater. The top surface of saltwater zone is detected at depths range from 10 m to 50 m in the coastal strip, and deepens toward the east into more than150 m. In extensive agricultural areas (Al Bolaily area) the depth to saltwater zone is found at relatively greater depth

(~200 m). Groundwater contamination by saline water from the sea is considered as a result of over pumping in the cultivated area.

## References


**Dahlin,** (1996**).** 2D resistivity surveying for environmental and engineering applications. First Break, 147, 275-283.

**De Breuk, W.** and **De Moor, G.** (1969). The water table aquifer in the eastern coastal area of Belgium. *Bull. Assoc. Sci. Hydro*. **14:** 137-155.

**DHV Consulting Engineers.** (1983**).** *Wadi Rasyan project. Final report*. Vol. **1.** Main report, prepared for TDA and the comm. of the European communities. DHV, Amesfoort, the Netherlands.

**DHV Consulting Engineers.** (1986). *Tihama basin water resources study report*. Vol. **1**, and Vol.2. DHV, Amesfoort, the Netherlands.

**DHV Consulting Engineers.** (1988**).** *Tihama basin water resources study*. Main report, DHV, Amesfoort, the Netherlands.

**Ebrahem A.A.M., Senosy M.M.,** and **Dahab K.A.** (1977). Geoelectrical and hydrochemical studies for delineating ground water contamination due to salt water intrusion in the northern part of the Nile delta, Egypt. *Ground Water Jour*., **352:** 216-222.

**El-Eryani., M.L.** (1979). Hydrogeology and groundwater potential of the Tihama *YAR, University Arizona, USA*.

**Flanzenbaum, J.,** (1986**).** Evaluation of saltwater intrusion into the Coastal Aquifer of Southern Virginia. *M.Sc. Thesis*, Virginia Univ. press, 141 p.

**Frohlich, R.K., Urish, D.W., Fuller, J.** and **Reilly, M.O. (**1994). Use of geoelectrical method in groundwater pollution surveys in a coastal environment. *Applied Geophysics. Jour. Int.,* **32:** 139-154.

**Geoscan M.** (2001) IPI2win program for 1D automatic and manual interpretation of VES curves, Russia, Moscow, Moscow State University, Geological Faculty, Department of Geophysics.

**Geukens F.** (1966) Geology of the Arabian Peninsula: a review of the geology of Yemen, (translated from the French by S.D.Bowers). *Prof. Pap. U.S. Geological Survey*, **560-B:** 23. Washington.

**Golden Software,** (1994**).** *Surfer for Windows*: Contouring and 3D surface Mapping, Golden, CO.

**Goodell, H.G. (**1986). A study of saltwater intrusion into the surface aquifer and the underlying of Yorktown Aquifer of Coastal Virginia. *Final Report* to *Virginia Environmental Endowment Richmond, VA*, 14 p.

**Griffiths, D.H.** and **Barker, R.D. (**1993**).** Two-dimensional resistivity imaging and modelling in areas of complex geology. *Applied Geophysics. Jour. Int.,* **29:** 211-226.

**Gun A.M.V.,** and **Ahmed A.A.** (1985). The water resource of Yemen. A summary and digest of available information. *TNO Institute of Applied Geosciences*, 2600 JA. Delft, the Netherlands.

**Hem J.D.,** (1989).. Study and interpretation of the chemical characteristics of natural water, 3rd edition. *U.S. Geological Survey, Washington, DC, Water-Supply Paper*, **2254**, 263p.

**Nowroozi, A.A., Stephen B. H.** and **Peter H.** (1999). Saltwater intrusion into the freshwater aquifer in the eastern shore of Virginia: a reconnaissance electrical resistivity survey. *Applied Geophysics. Jour. Int.,* **42:** 1: 1-22.

**Parasnis D.S.** (1986). Principle of Applied Geophysics. Chapman & Hall, London, 402 p.

**Rybakov S.V.,** and **Tkachenko R.I.** (1995). Groundwater resources available for development. Sanaa. Yemen.

**TS-HWC-UNDP/DESD** (1992). Technical Secretariat of the High Water Council. *Final reports*. Volume III: Surface water resources; Volume IV: *Groundwater resources*; Volume VI: Water supply, wastewater and sanitation.

**Urish D.W.** and **Frohlich R.K.** (1990). Surface electrical resistivity in coastal groundwater exploration. *Geoexploration. Jour. Int.,* **26:** 267-289.

**Van Overmeeren, R.A.** (1985**).** Water Resources of Wadi Surud Area. Geoelectrical investigation. Report WARY-42.

**Van Overmeeren R.A.** (1989). Aquifer boundaries explored by geo-electrical measurements in the coastal plains of Yemen. A case of equivalence. *Geophysics. Jour. Int.*, **54**: 38-48.

**Yemen National Census,** (2004**).** Population and housing census, Yemen Central Statistics Office, December 2004. *Ministry of Planning and Development.*

**Zohdy, A.A.R., (**1989**).** A new method for the automatic interpretation of Schlumberger and Wenner sounding curves. *Geophysics. Jour. Int.,***54**(2): 245-253.

**Zohdy, A.A.R., Martin, P.** and **Bisdorf, R.J. (**1993**).** A study of seawater intrusion using direct current soundings in the southeastern part of the Oxnard Plain, California. *Open-File Report* **93**-524. *U.S. Geological Survey,* 139 p.

# استقصاء نطاق اختراق مياه البحر في منطقة المخا–ساحل البحر الأحمر– اليمن باستخدام قياسات المقاومة الكهربائية

**أحمدعبد العزيزعبد القادر و محمود محمد سنوسي***

*أستاذ مساعد جيولوجيا المياه، قسم الجيولوجيا، كلية العلوم، جامعة تعز، اليمن*

** أستاذ الجيوفيزياء، قسم الجيولوجيا ،كلية العلوم ،جامعة أسيوط ، مصر*

*المستخلص.* تعتبر منطقة المخا من أقدم وأهم الموانئ اليمنية، إلا أنها تعاني من نقص شديد في إمدادات المياه العذبة نتيجة تلوث المصادر الجوفية باختراق مياه البحر. وقد دُرست هذه المشكلة باستخدام طريقتين – الجس الكهربائي العمودي – والتصوير ثنائي البعد للمقاومة الكهربائية، حيث نفذت عشر جسات كهربائية عمودية في المناطق البعيدة عن الساحل وأربعة خطوط من قياسات المقاومة الكهربائية ثنائية البعد في الحزام الساحلي .

بعد تحليل وتفسير القياسات الحقلية ومقارنتها بالمعلومات الجيولوجية والبيانات الهيدروجيولوجية، تبين وجود خزانين: الأول سطحي يمثل خزان رواسب الوديان الرباعي العلوي المكون من الحصى والرمل الخشن والناعم متقاطعة مع طبقات من الطين ، بسمك يصل إلى ٧٠ متراً والخزان الثاني عميق ويتكون أيضا من رواسب الوديان الرباعية ولكن أقل حجماً وأكثر تماسكاً من الرواسب العلوية، ويمتد من السطح بالقرب من الساحل وحتى عمق ٢٥٠ متراً تحت مستوى سطح البحر، كما دلت نتائج الدراسة على اختراق مياه البحر لهذا الخزان، حيث تبين أن النطاقات المشبعة بمياه البحر توجد على أعماق قريبة من السطح (١٠ متر) بالقرب من الشاطئ وتزداد

عمقا كلما ابتعدنا من الشاطئ حتى تصل إلى أكثر من ١٥٠ متراً عند مسافة ١٠ كم، وقد لوحظ زيادة عمق نطاق التلوث بمياه البحر في منطقة تركز الآبار (حقل آبار البليلي)، وأُرجع ذلك لانخفاض المنسوب وتحول اتجاه جريان المياه الجوفية نحو تلك المنطقة، كما أن نطاق التلوث بالمياه المالحة يظهر بشكل متعرج موازيا لخط الشاطئ معتمدا على كمية وأماكن الضخ في المنطقة.